Reduced Carbohydrate Availability Enhances the Susceptibility of Arabidopsis toward *Colletotrichum higginsianum*[1][W][OA]

Timo Engelsdorf, Robin J. Horst[2], Reinhard Pröls, Marlene Pröschel, Franziska Dietz, Ralph Hückelhoven, and Lars M. Voll*

Division of Biochemistry, Friedrich-Alexander-University Erlangen-Nuremberg, D–91058 Erlangen, Germany (T.E., R.J.H., M.P., F.D., L.M.V.); and Division of Phytopathology, Technical University Munich, D–85350 Freising-Weihenstephan, Germany (R.P., R.H.)

Colletotrichum higginsianum is a hemibiotrophic ascomycete fungus that is adapted to Arabidopsis (*Arabidopsis thaliana*). After breaching the host surface, the fungus establishes an initial biotrophic phase in the penetrated epidermis cell, before necrotrophic growth is initiated upon further host colonization. We observed that partitioning of major leaf carbohydrates was shifted in favor of sucrose and at the expense of starch during necrotrophic fungal growth. Arabidopsis mutants with impaired starch turnover were more susceptible toward *C. higginsianum* infection, exhibiting a strong negative correlation between diurnal carbohydrate accumulation and fungal proliferation for the tested genotypes. By altering the length of the light phase and employing additional genotypes impaired in nocturnal carbon mobilization, we revealed that reduced availability of carbon enhances susceptibility in the investigated pathosystem. Systematic starvation experiments resulted in two important findings. First, we showed that carbohydrate supply by the host is dispensable during biotrophic growth of *C. higginsianum*, while carbon deficiency was most harmful to the host during the necrotrophic colonization phase. Compared with the wild type, the increases in the total salicylic acid pool and camalexin accumulation were reduced in starch-free mutants at late interaction stages, while an increased ratio of free to total salicylic acid did not convey elevated pathogenesis-related gene expression in starch-free mutants. These observations suggest that reduced carbon availability dampens induced defense responses. In contrast, starch-free mutants were more resistant toward the fungal biotroph *Erysiphe cruciferarum*, indicating that reduced carbohydrate availability influences susceptibility differently in the interaction with the investigated hemibiotrophic and biotrophic fungal pathogens.

For successful establishment in their host plants, biotrophic and hemibiotrophic fungi have to gain access to nutrients from living host cells, thereby effectively evading the host defense system (for review, see Mendgen and Hahn, 2002; Divon and Fluhr, 2007; Münch et al., 2008). While the initiation and development of early infection structures are supported by the mobilization of lipids and carbohydrates stored in fungal spores of both hemibiotrophs and biotrophs (Thines et al., 2000; Both et al., 2005), fungal proliferation is driven by nutrient supply from the host tissue. Shortly after penetration of the first host cell, nutrient deprivation is established by the formation of specialized hyphae inside the invaded cells. During biotrophy, an interface between the fungal and the host plasma membrane is formed, through which solute exchange and effector delivery to the host takes place (for review, see Divon and Fluhr, 2007; Stergiopoulos and de Wit, 2009). Evidence obtained for the rust fungus *Uromyces fabae* suggests that host assimilates are mainly taken up in the form of hexoses generated from secreted fungal invertase and amino acids (Voegele et al., 2001; Struck et al., 2002, 2004). Recently, a high-affinity Suc transporter from the corn smut fungus *Ustilago maydis* was described that suggests a direct uptake of Suc in this pathosystem (Wahl et al., 2010).

Little is known about the role of plant primary metabolism in defense against pathogen attack. However, recently, three metabolic genes were identified that convey immunity to adapted pathogens. It has been found that transcriptional induction of the rice (*Oryza sativa*) Suc uniporter OsSWEET11 is triggered by the transcriptional activator-like effector PthXo1 of the hemibiotrophic bacterial phytopathogen *Xanthomonas oryzae* pv *oryzae*, providing the pathogen with extra Suc (Chen et al., 2010, 2012). Mutation of the OsSWEET11 promoter or the DNA recognition motif

[1] This work was supported by the Deutsche Forschungsgemeinschaft via the priority program FOR 666.

[2] Present address: Department of Biology, University of Washington, Seattle, WA 98195.

* Corresponding author; e-mail lvoll@biologie.uni-erlangen.de.

The author responsible for distribution of materials integral to the findings presented in this article in accordance with the policy described in the Instructions for Authors (www.plantphysiol.org) is: Lars M. Voll (lvoll@biologie.uni-erlangen.de).

[W] The online version of this article contains Web-only data.

[OA] Open Access articles can be viewed online without a subscription.

www.plantphysiol.org/cgi/doi/10.1104/pp.112.209676

of the transcriptional activator-like effector resulted in incompatibility between bacteria and infected rice plants (Chen et al., 2010). Second, Arabidopsis (*Arabidopsis thaliana*) plants accumulating high contents of Thr due to mutations in either Asp kinase or dihydrodipicolinate synthase were rendered highly resistant toward the adapted biotrophic oomycete pathogen *Hyaloperonospora arabidopsidis*, presumably because Thr or one of its downstream products is toxic toward *H. arabidopsidis* (Stuttmann et al., 2011).

Besides these two reports that describe the dependence of compatibility on only one metabolic gene, several other metabolic functions have been identified to date that influence compatibility quantitatively. It has been shown that several enzymes of plant primary metabolism, Glc-6-P dehydrogenase (Scharte et al., 2005), malic enzyme (Parker et al., 2009; Voll et al., 2012), and Pro dehydrogenase (Cecchini et al., 2011), provide the cytosol with reducing equivalents that are required for the effective production of reactive oxygen species and can directly support induced plant defenses with reducing power. In addition, several reports reinforce the ideas that (1) the balance between extracellular Suc and hexose is perceived by the host (Biemelt and Sonnewald, 2006, and refs. therein) and (2) the cellular redox status is seized by the plant (Foyer and Noctor, 2005, and refs. therein). Both metabolic processes are commonly affected after pathogen ingress and produce signals modulating the strength of the salicylic acid (SA)-dependent host defense response (Herbers et al., 1996; Pavet et al., 2005).

For instance, cleavage of Suc and diversion of hexoses as a carbon source for apoplast-resident pathogens shifts the apoplastic Suc-to-hexose ratio in favor of hexose. This represents a signal to induce host-encoded extracellular invertase that will further enhance the production of hexoses. In turn, elevated hexose reuptake into the symplast that occurs under these conditions enhances SA-based defense responses that will ultimately include the hypersensitive response (HR), as described by Biemelt and Sonnewald (2006). Likewise, diminished scavenging of reactive oxygen species also represents a trigger for SA responses and HR (Pavet et al., 2005; Chaouch et al., 2010).

To date, there is some experimental evidence that the effectiveness of the plant defense response depends on sufficient carbon supply to host cells. Elevated oxidative stress prevailing in the photorespiratory Arabidopsis *shmt* mutant with reduced mitochondrial Ser hydroxymethyltransferase activity leads to constitutive activation of pathogenesis-related (PR) genes and other defense responses (Moreno et al., 2005). Nevertheless, the *shmt* mutant is more susceptible to pathogen attack, as an additional boost of defense cannot be achieved upon challenge with pathogens (Moreno et al., 2005). This indicates the existence of a cross talk between primary metabolism and defense responses in the *shmt* mutant: it can be assumed that a limitation of central primary metabolism negatively impacts the host defense in the mutant, thereby overriding the constitutive positive effect caused by disturbed redox balance. Carbon limitation in *shmt* is caused by feedback inhibition of the Calvin cycle due to elevated photorespiration and the accompanying diminished capacity for the assimilation of carbohydrates. Vice versa, the Arabidopsis *cat2* mutant, lacking peroxisomal catalase and displaying increased vulnerability to oxidative stress, exhibits a heightened SA-based defense response compared with the wild type in long-day conditions only, when building blocks and carbohydrates are abundant, but not in short-day conditions, when the carbohydrate budget is more limiting (Chaouch et al., 2010). Furthermore, a recent study by Wang et al. (2011) revealed that the amplitude of induced plant defense responses is regulated by the circadian clock and that it is highest during the anticipated light phase, when carbon building blocks are abundant.

Colletotrichum higginsianum is a hemibiotrophic ascomycete fungus that was isolated from *Brassica rapa* and exhibits the closest relation to *Colletotrichum destructivum* isolates (O'Connell et al., 2004). *C. higginsianum* is adapted to Arabidopsis, as basal defense responses were found to be less pronounced compared with nonadapted relatives of the genus *Colletotrichum* (Shimada et al., 2006). Of 116 Arabidopsis ecotypes tested by Birker et al. (2009), 47% were susceptible toward *C. higginsianum*, including the ecotype Columbia (Col-0) studied here. Very recently, the first-draft genome sequence of *C. higginsianum* became available (O'Connell et al., 2012).

Leaf infections with *C. higginsianum* are initiated by conidia that land on the leaf surface and produce germ tubes, which then differentiate dome-shaped appressoria (for review, see Mendgen and Hahn, 2002; Münch et al., 2008; for an overview of the life cycle of *C. higginsianum*, see Supplemental Fig. S1). Compatible solutes are accumulated inside the appressorium during its maturation, while appressorial cell walls melanize, leading to the establishment of high turgor pressure in the presence of external water supply. The wall of the underlying epidermis cell is subsequently pierced by a penetration peg with a combination of mechanical force and lytic enzyme activities (Bechinger et al., 1999; Deising et al., 2000). In the penetrated host epidermis cells, *C. higginsianum* establishes itself as a biotroph within 36 h post inoculation by forming a bulbous infection vesicle that produces lobed biotrophic primary hyphae. These biotrophic structures are surrounded by interfacial bodies and the host plasma membrane (Kleemann et al., 2012). Upon the subsequent colonization of neighboring cells at around 72 h post inoculation, a switch in both hyphal morphology and life style occurs. Narrow-bore necrotrophic secondary hyphae grow rapidly, which eventually leads to necrotic lesions on the infected leaves that are visible shortly after the switch to necrotrophy. In the macerated tissue, new conidiospores are formed mitotically at the base of pin-shaped setae in structures called acervuli.

In this study, we have analyzed the role of major leaf carbohydrate metabolism of Arabidopsis and the importance of carbohydrate availability in the host tissue for the interaction with *C. higginsianum*. Experiments employing mutants with impaired leaf carbohydrate metabolism in different light/dark cycles demonstrated that a shortage in host carbohydrate availability enhances susceptibility to the fungus. Systematic starvation experiments further revealed that *C. higginsianum* does not depend on carbohydrate supply by the host during biotrophic growth, while carbohydrate limitation of the host impairs the induced host defense responses and increases susceptibility to *C. higginsianum* during necrotrophic colonization.

RESULTS

Starch Turnover Is Altered during Necrotrophic Growth of *C. higginsianum*

In a broad range of pathosystems, dynamic changes in major carbohydrate metabolism occur during the interaction with leaf pathogens, which are regarded as a consequence of metabolic reprogramming by the microbial invaders upon successful establishment (Chou et al., 2000; Fotopoulos et al., 2003; Berger et al., 2004; Swarbrick et al., 2006; Doehlemann et al., 2008; Horst et al., 2008). Ultimately, leaves colonized by biotrophic pathogens will undergo a local source-to-sink transition due to the diversion of nutrients by the pathogen (Biemelt and Sonnewald, 2006).

In order to characterize changes in host primary metabolism of Arabidopsis leaves during both the biotrophic and necrotrophic interaction phases with the hemibiotroph *C. higginsianum*, we first analyzed steady-state contents of major leaf carbohydrates (Fig. 1) in the wild type (Col-0). In the course of *C. higginsianum* infection (Supplemental Fig. S1), soluble sugars progressively accumulated in comparison with mock control leaves (Fig. 1, A and B), whereas a reduction in transitory starch accumulation coincided with the occurrence of necrotic lesions on infected leaves at around 3.5 d post infection (dpi; Fig. 1C). In addition, a pulse-chase experiment (see Supplemental Materials and Methods S1) demonstrated that carbon flux into the starch pool and out of the soluble sugar and amino acid pools was slowed down in infected leaves compared with controls (Supplemental Fig. S2). Consequently, a significantly higher proportion of ^{14}C label remained in the neutral sugar fraction in infected leaves compared with controls (Supplemental Fig. S2). While overall starch turnover was substantially reduced with the onset of the necrotrophic colonization phase, an accumulation of starch around early necrotic lesions at 3.5 dpi occurred, which disappeared upon further expansion of the necrosis from 4.5 dpi onward (Fig. 1D).

These observations prompted us to examine the photosynthetic performance of infected leaves with necrotic symptoms in spatial resolution during the light phase between 3.5 and 4 dpi. While the electron transport rate was reduced adjacent to necrotic spots, it was increased in unaffected leaf areas compared with mock-infected leaves (Supplemental Fig. S3, A and B). The increase in uncontrolled energy dissipation correlated positively with the proximity to necrosis, indicating that, in addition to starch turnover,

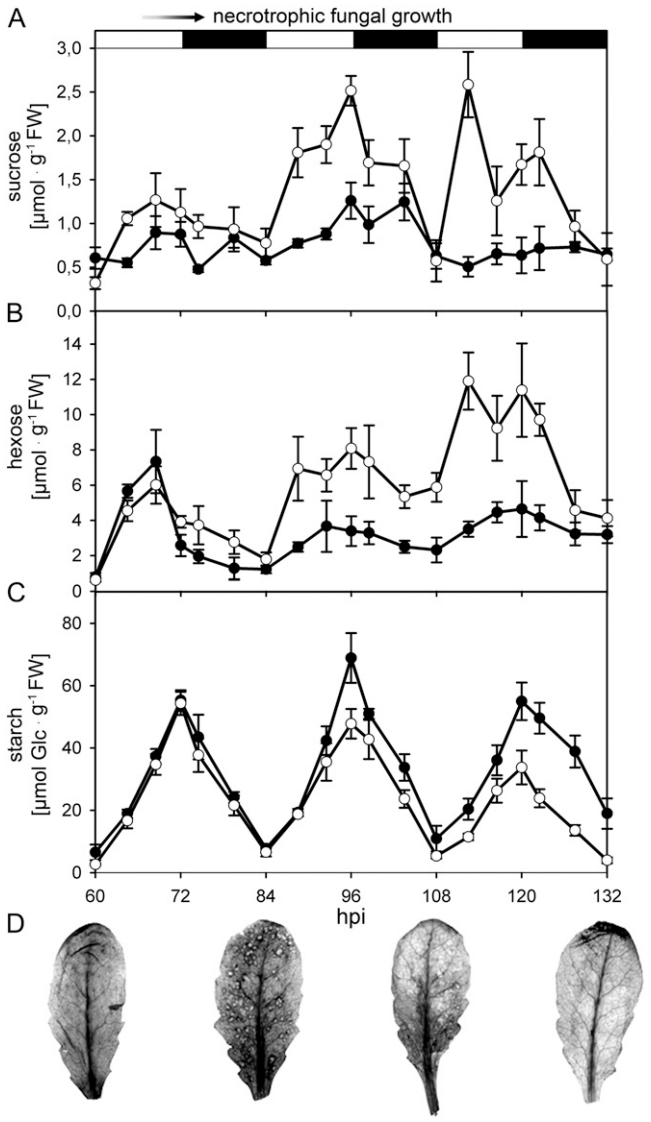

Figure 1. Diurnal changes of carbohydrate content in Arabidopsis leaves after infection with *C. higginsianum*. A to C, The contents of Suc (A), hexose (B), and starch (C) in fully expanded *C. higginsianum*-infected (white circles) and mock control (black circles) leaves from 5-week-old plants grown in a 12-h/12-h light/dark cycle were determined between 2.5 dpi (60 h post infection [hpi]) and 5.5 dpi (132 hpi). The light/dark phases are indicated above the graphs by white and black bars, respectively. Spray inoculation with *C. higginsianum* conidia was conducted 30 min before lights off at day 0. The onset of necrotrophic fungal growth around 60 to 72 hpi is indicated at the top. FW, Fresh weight. D, Local starch accumulation in *C. higginsianum*-infected leaves visualized by iodine staining at the end of the dark phase (corresponding to 60, 84, 108 and 132 hpi). Error bars represent SE ($n = 4$).

necrotrophic growth disturbs the integrity of photoautotrophic leaf metabolism (Supplemental Fig. S3, C and D).

Mutants with Impaired Starch Metabolism Are Hypersusceptible toward *C. higginsianum*

The physiological characterization of *C. higginsianum*-infected Arabidopsis leaves indicated that starch turnover is disturbed during necrotrophic growth of the pathogen. Therefore, we assessed whether susceptibility toward *C. higginsianum* is affected in mutants with altered starch turnover. To this end, we determined fungal genomic DNA quantity by quantitative PCR (qPCR) at different time points post infection and compared fungal proliferation in the starch-free mutants *phosphoglucomutase-1* (*pgm*) and *ADP-glucose pyrophosphorylase1-1* (*adg1-1*; Caspar et al., 1985; Lin et al., 1988) with the starch-excess mutant *starch excess1-1* (*sex1-1*), which is hampered in starch degradation (Caspar et al., 1991; Yu et al., 2001), as well as with *triose-phosphate/phosphate translocator1-2* (*tpt1-2*), a mutant in which triose-phosphate export from the chloroplast is abolished (Schneider et al., 2002; Supplemental Fig. S4). The plants were grown in a 12-h-light/12-h-dark cycle to minimize growth differences between the genotypes. Infection experiments were conducted at the end of the vegetative phase. The increase in fungal DNA content was negligible until the onset of necrotrophic growth at around 3 dpi (Fig. 2A). Compared with the wild type at 4 dpi, fungal colonization was increased more than 3-fold in all mutants with disturbed starch metabolism but not in the *tpt1-2* mutant (Fig. 2A), indicating that starch metabolism plays an important role for compatibility in the Arabidopsis-*C. higginsianum* interaction.

Altered carbohydrate metabolism in the starch-free mutants could influence the interaction with the hemibiotroph *C. higginsianum* by two possible means.

First, *pgm* and *adg1-1* lack a transitory starch buffer (Fig. 3A), which leads to periodic starvation of mutant leaves toward the end of each dark phase (Caspar et al., 1985; Lin et al., 1988; Thimm et al., 2004).

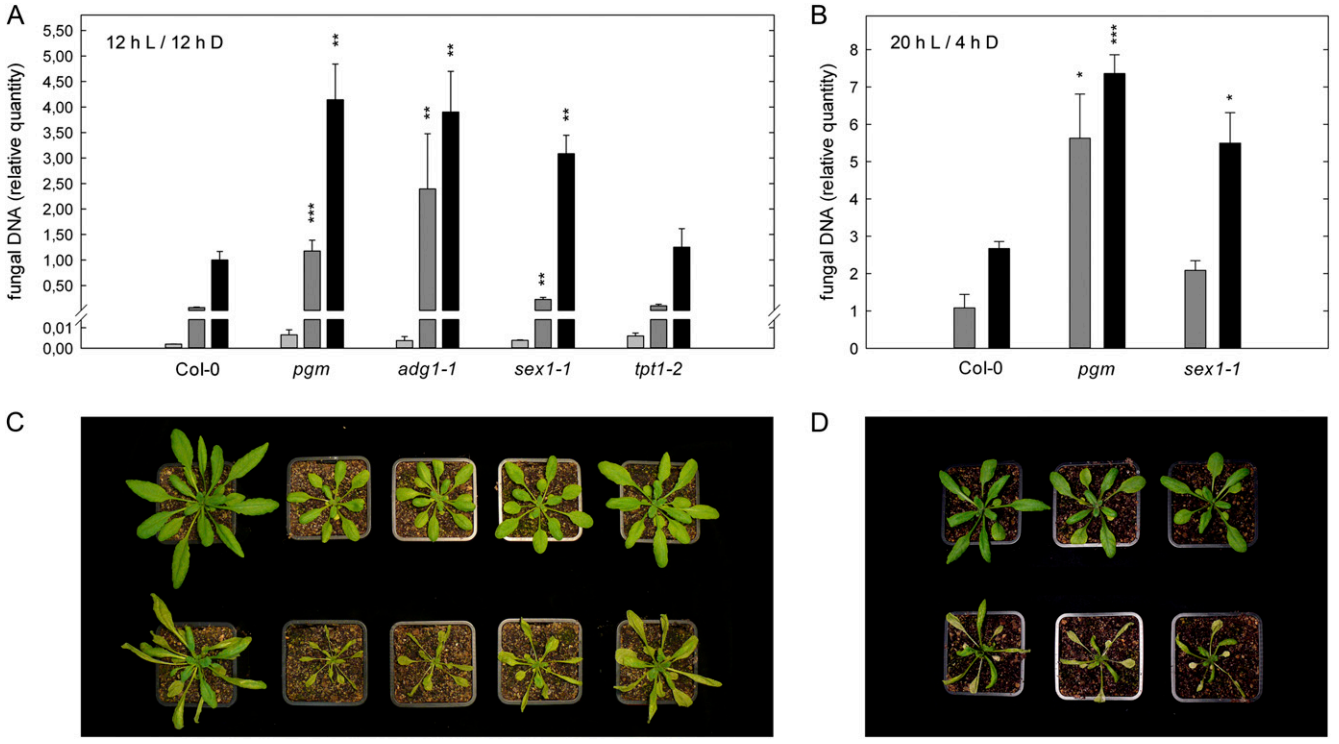

Figure 2. Susceptibility of Arabidopsis mutants of central carbohydrate metabolism toward *C. higginsianum*. A and B, Five-week-old plants in 12-h/12-h light/dark cycles (A) and 4-week-old plants in 20-h/4-h light/dark cycles (B) were infected with *C. higginsianum* at the end of the vegetative growth phase in each condition. As a measure of fungal proliferation, the relative quantity of fungal genomic DNA was determined by qPCR in leaves harvested at 2 dpi (light gray bars), 3 dpi (dark gray bars), and 4 dpi (black bars). Genotypes are indicated below the graphs. Values are means of three biological replicates measured in three technical replicates ± SE from one representative experiment. For each replicate, leaves were pooled from two separate plants, and quantitation data were normalized to Col-0 at 4 dpi in 12-h/12-h light/dark cycles. For most genotypes, the experiment was repeated more than six times. Asterisks indicate significant differences from Col-0 ($^*P < 0.05$, $^{**}P < 0.01$, $^{***}P < 0.001$, Student's *t* test). C and D, Disease symptoms and growth phenotypes of infected plants in 12-h/12-h light/dark cycles (C) and 20-h/4-h light/dark cycles (D) at 4 dpi (bottom row) compared with noninfected plants of the same age (top row).

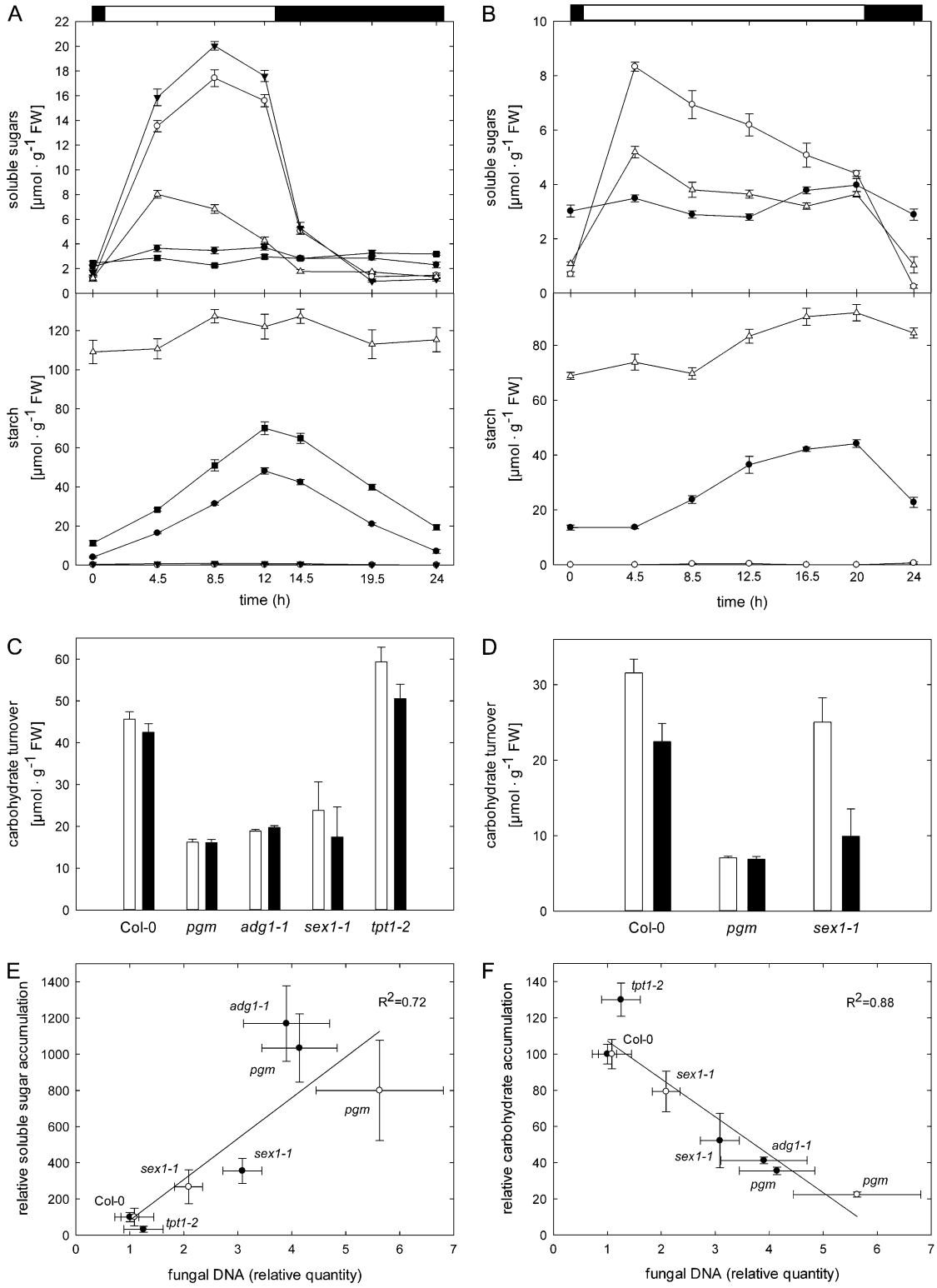

Figure 3. Diurnal accumulation and turnover of carbohydrates in Arabidopsis mutants affected in major leaf carbohydrate metabolism. A and B, Soluble sugar and starch contents of untreated leaves were monitored in 12-h/12-h light/dark cycles (A) and 20-h/4-h light/dark cycles (B) in the indicated Arabidopsis genotypes over a 24-h diurnal cycle. Col-0, black circles; *pgm*, white circles; *adg1-1*, black triangles; *sex1-1*, white triangles; *tpt1-2*, black squares. Values are means of four biological replicates ± SE. C and D, The diurnal carbohydrate turnover in 12-h/12-h light/dark cycles (C) and 20-h/4-h light/dark cycles (D) was calculated from the data depicted in A and B, respectively. Carbohydrate accumulation, white bars; carbohydrate

Consequently, the reduced diurnal carbohydrate supply in mutant leaves could, in turn, impair the provision of carbon building blocks for the host defense response. Alternatively, *C. higginsianum* might benefit from an about 10-fold increased accumulation of free soluble sugars in *pgm* and *adg1-1* during the light phase (Fig. 3A). As outlined in the introduction, it has been demonstrated that the availability of soluble sugars can be an important compatibility factor in biotrophic interactions (Chen et al., 2010).

In support of the first hypothesis, the total diurnal carbohydrate turnover in uninoculated leaves was reduced to a similar extent in mutants with compromised starch metabolism, *pgm*, *adg1-1*, and *sex1-1*, in comparison with wild-type and *tpt1-2* leaves (Fig. 3C). To further test whether the duration of carbohydrate shortage during the dark phase affects susceptibility, we infected Arabidopsis plants with *C. higginsianum* in extended long-day conditions with a 20-h light period and a 4-h dark period. In this regime, all genotypes grew to a comparable rosette size, thereby minimizing pleiotropic effects (Fig. 2D). Four-week-old plants were challenged with pathogen, which represents the end of the vegetative phase in these growth conditions. In these extended long-day conditions, nocturnal starvation of *pgm* was substantially shortened in comparison with 12-h/12-h light/dark cycles (Fig. 3B), but the total carbohydrate turnover in *pgm* remained invariably low compared with the wild type (Fig. 3D). In *sex1-1*, the starch accumulation rate exceeded the starch mobilization rate, as the mutant plants had not yet reached the storage capacity for starch at the point of harvest. Nevertheless, *sex1-1* exhibited a similar decrease of nocturnal carbohydrate mobilization to the *pgm* mutant (Fig. 3D).

The progress of fungal infection was accelerated in 20-h/4-h light/dark cycles in comparison with 12-h/12-h light/dark cycles (please note that the numbers in Figure 2, A and B, are normalized to the same reference). *C. higginsianum* colonization at 3 dpi was increased in *pgm* and *sex1-1* by 5- and 2-fold relative to the wild type, respectively, similar to the situation in the 12-h/12-h regime at 4 dpi (compare Fig. 2, A and B). Therefore, we can exclude that the length of the dark phase and the associated carbon shortage represent a susceptibility factor in the *pgm* mutant. Instead, the extent of diurnal carbon turnover appears to determine susceptibility.

In support of this interpretation, the diurnal carbohydrate accumulation in the respective genotypes showed a negative correlation with the degree of susceptibility in both light regimes (Fig. 3F, with data calculated from Fig. 2A and Fig. 3C for 12-h/12-h light/dark [black circles] and data calculated from Fig. 2B and Fig 3D for 20-h/4-h light/dark [white circles]). However, the foliar accumulation of soluble sugars during the light phase also exhibited a positive correlation with susceptibility toward *C. higginsianum* in both the 12-h/12-h and the 20-h/4-h experiments (Fig. 3E, with data calculated from the values displayed in Fig. 2, A and B, and Fig. 3, A and B, respectively). These correlations were evident, whether the carbohydrate accumulation data of untreated leaves (Fig. 3, E and F, black circles) or the corresponding water-treated control plants (Supplemental Figs. S5 and S6) were plotted. A reasonable correlation of susceptibility with specific changes in individual soluble carbohydrates caused by *C. higginsianum* infection was absent (Supplemental Fig. S7, A–D), as *C. higginsianum* infection caused similar changes to major soluble carbohydrates in all genotypes we examined (Supplemental Fig. S5). In light of the presented correlations, it remains ambiguous whether the elevated susceptibility in mutants with impaired starch turnover is caused by reduced carbohydrate turnover or by increased soluble sugar availability.

Carbon Starvation Increases Susceptibility toward *C. higginsianum*

In a comprehensive study by Usadel et al. (2008), it has been shown that starvation for carbon can be induced in the wild type by extending the dark period for more than 8 to 12 h. In order to resolve whether total soluble sugar abundance might account for increased susceptibility, we induced carbohydrate starvation in Col-0, *pgm*, *adg1-1*, and *sex1-1* by extending the dark phase after infection with *C. higginsianum* for 24 or 48 h, thereby eliminating one or two ensuing light phases, respectively, before leaf samples were harvested for fungal quantitation at 3.5 dpi (Fig. 4A, top two rows). We confirmed that total carbohydrate storage (i.e. the sum of soluble sugars and starch) is depleted in *pgm* and *adg1-1* before the end of the regular dark phase in our growth conditions (Fig. 3A). In dark-incubated Col-0, the transitory starch pool was exhausted during the first anticipated light phase (Supplemental Table S1).

Fungal proliferation in the necrotrophic phase at 3.5 dpi was already increased by about 2-fold in *pgm* and *adg1-1* after one darkened light phase (DLP), while a

Figure 3. (*Continued.*)
degradation, black bars. Values are means of four biological replicates ± SE. FW, Fresh weight. E and F, Correlation analysis of relative soluble sugar (E) and total major carbohydrate (F; soluble sugar + starch) accumulation during the light phase in 12-h/12-h light/dark cycles (black circles) and 20-h/4-h light/dark cycles (white circles) with the indicated relative quantities of genomic C. higginsianum DNA. Values for fungal proliferation were taken from Figure 2A (12-h/12-h light/dark) and Figure 2B (20-h/4-h light/dark). All carbohydrate data were calculated as percentages of the respective wild-type values depicted in A and B, respectively. Similar correlations were obtained when carbohydrate data from mock-treated plants (Supplemental Fig. S5) instead of uninfected control plants (Supplemental Fig. S6, A and B) were used.

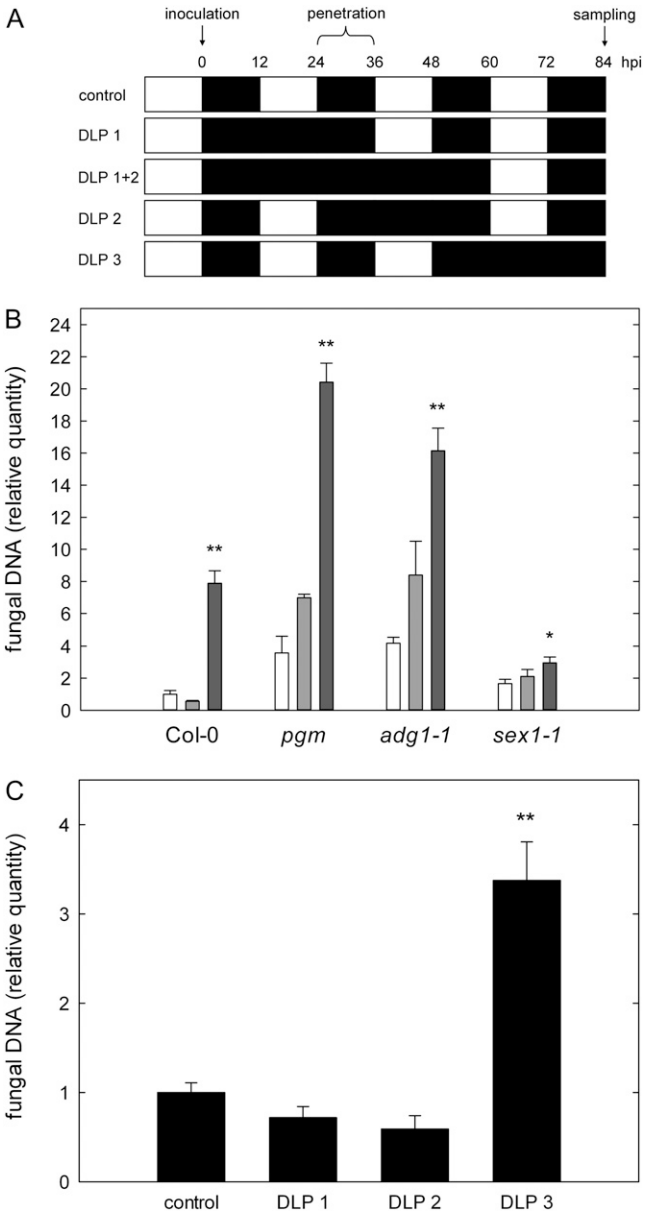

Figure 4. Susceptibility toward *C. higginsianum* after dark-induced starvation. Plants were dark incubated after infection with *C. higginsianum*, and the relative quantity of fungal genomic DNA was determined by qPCR in leaves harvested at 3.5 dpi (84 h post infection [hpi]). A, Schematic overview of the combinations of DLP applied after the infection. The relative time of fungal penetration and sampling after inoculation is indicated above as a time scale. B, Relative quantity of fungal genomic DNA in leaves of Col-0, *pgm*, *adg1-1*, and *sex1-1* at 3.5 dpi. Control (12-h/12-h light/dark), white bars; DLP 1, light gray bars; DLP 1+2, dark gray bars. C, Col-0 control compared with Col-0 with DLP 1, DLP 2, and DLP 3. For each replicate, leaves were pooled from two separate plants. Values are means of three biological replicate pools measured in three technical replicates ± SE. Asterisks indicate significant differences between DLP samples and control samples (*$P < 0.05$, **$P < 0.01$, Student's *t* test).

4- and 8-fold increase in fungal proliferation was observed in the starch-free mutants and Col-0 upon darkening of two light phases (DLP 1+2), respectively (Fig. 4B). Due to a reduced starch mobilization rate, *sex1-1* was not starved for carbon in any of the selected conditions, as substantial amounts of starch were constantly detectable (Supplemental Table S1). Consequently, *sex1-1* exhibited only a small increase in susceptibility in extended darkness (Fig. 4B). Remarkably, these results demonstrate that the availability of free soluble sugars in the host leaf does not represent a prerequisite for efficient *C. higginsianum* proliferation, as fungal colonization of starved Col-0, *pgm*, and *adg1-1* leaves was increased upon carbon depletion in DLP conditions relative to carbohydrate-replete control leaves.

To test if the effect of carbon starvation on host susceptibility differs during specific phases of *C. higginsianum* colonization, we induced starvation at different time points after infection of Col-0 by darkening the first (DLP 1), the second (DLP 2), or the third (DLP 3) light phase after inoculation. Quantification of fungal proliferation at 3.5 dpi showed that colonization by *C. higginsianum* was substantially elevated when the third light phase was omitted, indicating that carbon shortage in host leaves is most detrimental during necrotrophic growth of the pathogen (Fig. 4C). It appears likely that a shortage for carbon compromises the host defense response and promotes susceptibility during the necrotrophic colonization phase. In contrast, dark-induced carbon shortage during the early, mainly biotrophic postpenetration phase did not increase susceptibility toward *C. higginsianum*.

Diurnal Carbohydrate Availability Represents a Susceptibility Factor

To obtain independent evidence that diurnal carbohydrate availability represents a susceptibility factor in the Arabidopsis-*C. higginsianum* interaction, we infected mutants that have the full enzymatic capacity for starch metabolism but were also reported to suffer from periodic nocturnal starvation due to other limitations.

First, we investigated *circadian clock associated1/late elongated hypocotyl* (*cca1/lhy*) double mutants that display an accelerated oscillation of the circadian clock, which leads to premature consumption of transitory starch and periodic starvation at the end of each dark period (Graf et al., 2010). We confirmed that the transitory starch pool was periodically exhausted in the *cca1/lhy* double mutants in the 12-h/12-h light/dark regime we applied (Supplemental Table S2). Second, we assessed Arabidopsis plants overexpressing maize (*Zea mays*) malic enzyme in the stroma (MEm4), which have reduced transitory malate and fumarate storage capacities and exhibit a reduced respiration rate as a consequence of carbon shortage at the end of the dark phase in short-day conditions only (Fahnenstich et al.,

2007; Zell et al., 2010). We confirmed that malate and fumarate accumulation during the light phase was reduced in MEm4 transgenics and that soluble sugar and starch contents were not notably altered compared with wild-type plants in our growth conditions (Supplemental Table S3).

Susceptibility toward *C. higginsianum* was strongly increased in both the *cca1/lhy* double mutants and the MEm4 transgenics in conditions of nocturnal carbon shortage (Fig. 5, A and B). Interestingly, the susceptibility of MEm4 plants toward *C. higginsianum* was only increased in short-day conditions (compare Fig. 5, B and C), when respiration rates at the end of the dark period were reported to be diminished in the transgenics (Zell et al., 2010).

Based on the presented data, we conclude that a reduction in diurnal carbon turnover and the associated limited nocturnal carbon availability increase susceptibility in the Arabidopsis-*C. higginsianum* interaction.

Induced Defense Responses Are Altered in Starch-Free Mutants

We analyzed major induced defense responses of the mutants *pgm*, *adg1-1*, and *sex1-1* in comparison with the wild type to assess whether the host defense response is dampened in mutants with reduced starch turnover. To this end, we focused on SA-dependent responses and camalexin accumulation, which are both necessary for an effective defense against *C. higginsianum* (Narusaka et al., 2004; O'Connell et al., 2004).

The amount of free SA was strongly elevated in the starch-free mutants, especially at 2 and 4 dpi (Fig. 6A). While only 10% of the total SA pool was conjugated as salicylic acid glucosides (SAG) in the starch-free mutants, more than 80% of the SA pool was still conjugated in the wild type at 4 dpi (Fig. 6A). In both starch-free mutants, the total SA pool (i.e. free SA plus SAG) was diminished by 40% compared with the wild type at 4 dpi. In *sex1-1*, the SA pool composition was similar to the wild type until 4 dpi, when 50% of the total SA was present as free SA in the mutant, representing an intermediate phenotype. In mock-treated plants of all genotypes, the amount of total SA was lower than 14 ng cm^{-2} at all time points.

Free SA is generally believed to be the active form for the induction of defense responses, while SAG is thought to either represent an SA reservoir or an inactivated form of the messenger (for review, see Vlot et al., 2009). As free SA and total SA contents were already elevated at 2 dpi in starch-free mutants compared with the wild type (Fig. 6A), we examined whether the frequency of HR was also increased. However, the occurrence of HR underneath *C. higginsianum* appressoria was not significantly different between the wild type (2.22% ± 0.38% of all appressoria elicited an HR), *pgm* (1.56% ± 0.36%), and *adg1-1* (1.35% ± 0.31%) during the early interaction, providing an indication that sensitivity toward SA might be reduced in the mutants. As another consequence of elevated free-SA levels, a stronger induction of SA-dependent PR genes would be expected in *pgm* and *adg1-1*. While PR-2 transcripts accumulated earlier in *pgm* and *adg1-1* than in the wild type, their amount were reduced at 4 dpi compared with the wild type and *sex1-1* (Fig. 6C). At 4 dpi, PR-1 transcripts were less abundant in the starch-free mutants relative to the wild type. In contrast, the jasmonate (JA)/ethylene (ET)-dependent PR genes PLANT DEFENSIN1.2 (PDF1.2) and PR-4 were induced earlier than the SA-responsive genes, but the accumulation of PDF1.2 and PR-4 transcripts was also reduced in *pgm* and *adg1-1* in comparison with the wild type until 4 dpi. Our results demonstrate that the transcriptional output of both the SA- and the JA/ET-triggered defense pathways is slightly dampened in the starch-free mutants.

We also analyzed the abundance of the major Arabidopsis phytoalexin camalexin, whose accumulation is only partly dependent on SA (for review, see

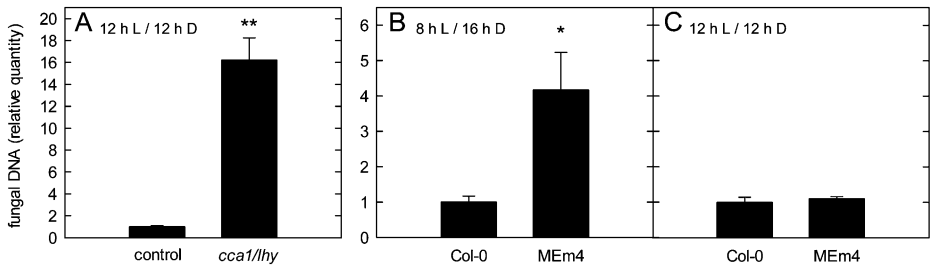

Figure 5. Susceptibility of Arabidopsis mutants with periodic carbon shortage toward *C. higginsianum*. A, Four-week-old *cca1/lhy* mutants and the corresponding control (see "Materials and Methods") were infected with *C. higginsianum* in 12-h/12-h light/dark cycles. The relative quantity of genomic fungal DNA was determined by qPCR in leaves harvested at 3 dpi. B and C, Transgenic MEm4 plants were grown in 8-h/16-h (B) and 12-h/12-h (C) light/dark cycles. Plants were infected at the age of 7 weeks (B) and 5 weeks (C), at the end of the respective vegetative growth phase, and the relative quantity of genomic fungal DNA was determined by qPCR in leaves harvested at 4 dpi. Values are means of three biological replicates measured in three technical replicates ± SE. For each replicate, leaves were pooled from two separate plants. Asterisks indicate significant differences from the respective control plants (*$P < 0.01$, **$P < 0.001$, Student's *t* test).

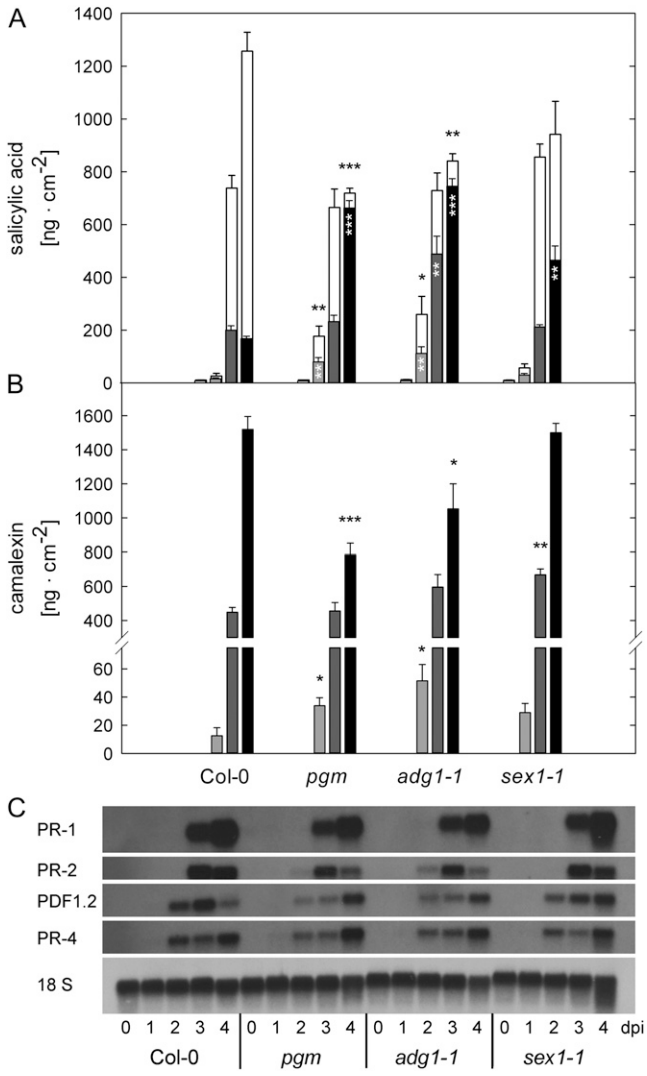

Figure 6. Induced defense responses in Arabidopsis mutants with impaired starch turnover after infection with *C. higginsianum*. A and B, Free SA (black and gray bars) and total SA (white bars; free SA + SAG; A) as well as camalexin contents (B) were analyzed at 1 dpi (pale gray bars), 2 dpi (light gray bars), 3 dpi (dark gray bars), and 4 dpi (black bars). Values are means ± SE ($n = 4$). Asterisks indicate significant differences from Col-0 (*$P < 0.05$, **$P < 0.01$, ***$P < 0.001$, Student's *t* test). C, Northern-blot analysis of *PR-1*, *PR-2*, *PDF1.2*, and *PR-4* transcript accumulation. Each lane was loaded with 8 μg of total RNA for samples taken at 0, 1, 2, 3, and 4 dpi with *C. higginsianum*.

Glawischnig, 2007). Camalexin was not detectable in all mock-treated leaves and in infected leaves until 1 dpi. At 2 dpi, the accumulation of camalexin was accelerated in *pgm* and *adg1-1*, whereas it was reduced in these two genotypes compared with the wild type at 4 dpi. In *sex1-1*, however, the camalexin amount was increased at 3 dpi but similar to the wild type at 2 and 4 dpi (Fig. 6B).

Taken together, our results demonstrate that the responsiveness of camalexin and SA accumulation is not generally reduced in the starch-free mutants but that the capacity to produce these compounds is limited compared with the wild type. Additionally, we have observed that the transcript accumulation of SA-dependent PR genes lags behind the accumulation of free SA in *pgm* and *adg1-1*.

Starch-Free Mutants Display Increased Resistance to the Biotrophic Fungus *Erysiphe cruciferarum*

In light of our results, we assessed the interaction of *pgm*, *adg1-1*, and *sex1-1* with the powdery mildew fungus *E. cruciferarum* in order to examine whether compatibility was similarly affected in the interaction with an obligate biotrophic fungus.

The proliferation of *E. cruciferarum* was significantly reduced on *pgm* and *adg1-1* and slightly reduced on *sex1-1* leaves (Fig. 7A). It has already been shown that

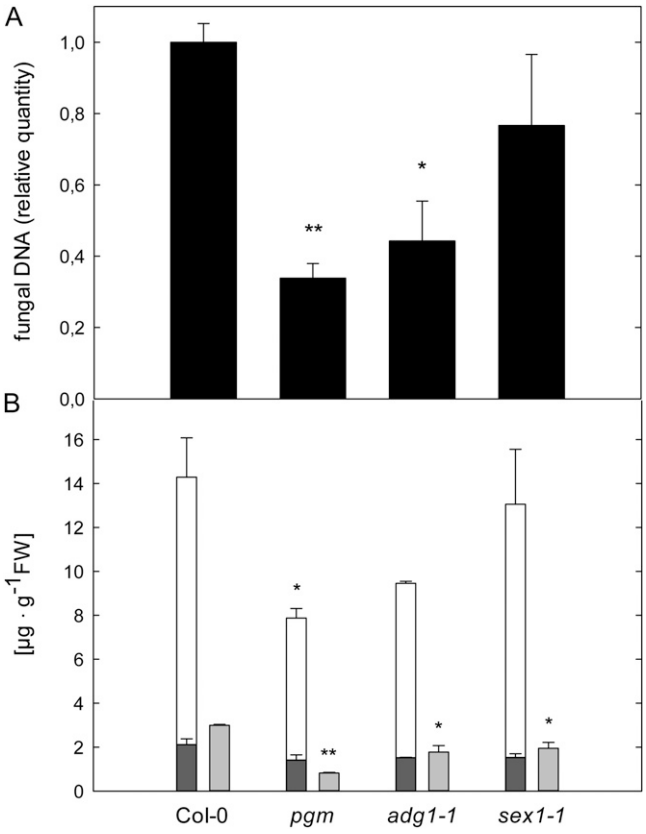

Figure 7. Susceptibility of Arabidopsis mutants with impaired starch turnover toward *E. cruciferarum*. A, The relative quantity of genomic *E. cruciferarum* DNA was determined by qPCR in leaves harvested at 6 dpi. Values are means of three biological replicates measured in three technical replicates ± SE. Asterisks indicate significant differences from Col-0 plants (*$P < 0.05$, **$P < 0.001$, Student's *t* test). B, Free SA (dark gray bars), total SA (white bars; free SA + SAG), and camalexin (light gray bars) contents at 6 dpi with *E. cruciferarum*. Values are means ± SE ($n = 3$). Asterisks indicate significant differences from Col-0 (*$P < 0.05$, **$P < 0.001$, Student's *t* test). Genotypes are indicated below the graphs. FW, Fresh weight.

carbohydrate availability in the host tissue is necessary for an efficient establishment of the barley (*Hordeum vulgare*) powdery mildew fungus (Jain et al., 2004), indicating that the decreased diurnal carbohydrate budget in starch-free mutants reduces susceptibility toward *E. cruciferarum*.

There was no substantial accumulation of free SA or camalexin in powdery mildew-infected leaves of any analyzed genotype (Fig. 7B), indicating a very efficient suppression of the host defense by the adapted pathogen *E. cruciferarum*. Nevertheless, the total pool size of the defense compounds SA and camalexin was still reduced in all three mutants compared with the wild type (Fig. 7B).

DISCUSSION

Reduced Diurnal Carbohydrate Turnover, and Not Increased Soluble Sugar Availability, Increases Susceptibility in the Arabidopsis-*C. higginsianum* Interaction

In the middle of the last century, the dependence of plant disease resistance on nutritional status was extensively investigated, leading to the classification into "high-sugar diseases" and "low-sugar diseases" (Horsfall and Dimond, 1957). However, this classification was not valid for all fungal pathosystems, and the molecular mechanisms behind the macroscopic phenomenon remained elusive.

Starch-free mutants display an increased accumulation of soluble sugars during the light phase, while in parallel, the diurnal carbohydrate availability is reduced relative to the wild type, making it difficult to extract which of the two associated changes in carbohydrate metabolism determines an increased susceptibility toward *C. higginsianum*. We present several lines of evidence that the diminished diurnal carbohydrate availability determines the elevated susceptibility of mutants affected in starch turnover. First, *pgm* and *sex1-1* remained hypersusceptible in extended long-day conditions (20-h/4-h light/dark) when the endogenous soluble sugar content in the mutants was reduced 2- to 4-fold during the light phase as compared with 12-h/12-h light/dark cycles. This indicates that the reduced diurnal carbohydrate turnover, which was similar in both growth conditions, and not the accumulation of soluble sugars accounts for the increased susceptibility of the mutants toward *C. higginsianum*. Second, mutant and wild-type plants became more susceptible in extended darkness when only minute amounts of soluble sugars were detectable in the leaves.

Third, we challenged two additional genotypes that suffer from periodic nocturnal starvation with *C. higginsianum*. The transitory storage of organic acids is reduced in MEm4 transgenics (Fahnenstich et al., 2007; Zell et al., 2010), while double mutants affected in the circadian clock regulators LATE ELONGATED HYPOCOTYL (LHY) and CIRCADIAN CLOCK ASSOCIATED1 (CCA1) exhibit a premature nocturnal depletion of the transitory starch pool due to an accelerated cycling of the circadian clock (Graf et al., 2010). Both genotypes also exhibited a strongly increased susceptibility toward *C. higginsianum*. Intriguingly, fungal proliferation in MEm4 transgenics was only increased in short-day conditions, when reduced organic acid storage affects nocturnal respiration (Zell et al., 2010). Thus, MEm4 transgenics display a conditional increase in susceptibility only when diurnal carbon turnover is diminished and nocturnal carbon shortage prevails.

Carbohydrate Supply to Biotrophic Hyphae Is Not Limiting for *C. higginsianum* Infection

In several interactions, it was shown that biotrophic phytopathogens rely on nutrient supply by the host for intracellular growth, which was most clearly demonstrated by the loss of compatibility between rice and *X. oryzae* pv *oryzae* when the pathogen-driven induction of Suc transporters was disabled (Chen et al., 2010, 2012). To date, it is not clear whether compatibility to hemibiotrophs depends on nutrient supply during the biotrophic colonization phase. It is commonly assumed that hemibiotrophs would benefit from carbohydrate abundance during their biotrophic growth phase as biotrophs do (for review, see Münch et al., 2008). However, only five of the 94 annotated sugar transporter genes in the *C. higginsianum* genome are preferentially expressed during the biotrophic phase (O'Connell et al., 2012).

In this study, we present evidence that compatibility toward *C. higginsianum* is not limited by carbohydrate supply from the host during the biotrophic phase. First, we have observed that three independent mutant genotypes with a shortage in diurnal carbon availability were hypersusceptible toward *C. higginsianum*. Second, the susceptibility of Arabidopsis wild-type plants and starch-free mutants was increased upon induction of carbohydrate shortage during the time of biotrophic growth (DLP 1+2). If carbohydrate supply to *C. higginsianum* was limiting during the biotrophic phase, we would expect an increased resistance in host plants grown in DLP 1+2 in comparison with control plants growing in regular diurnal light/dark cycles. However, we determined a low content of free Glc even after prolonged dark incubation of 72 h (data for up to 48 h of extended darkness are shown in Supplemental Table S1), which might be provided by the mobilization of carbohydrates from cell wall hemicelluloses, as reported by Lee et al. (2007). Nevertheless, it appears unlikely that the minute amounts of soluble Glc in the leaf tissue were sufficient to efficiently support *C. higginsianum* at an exclusively biotrophic colonization stage.

Evidence already exists that the appressorium of *Colletotrichum* spp. is necessary for the suppression of

induced defense responses like the indole glucosinolate pathway (Hiruma et al., 2010). Our data support the idea that the biotrophic interaction phase might be relevant for the suppression of host defense rather than for the acquisition of nutrients.

Carbon Availability Influences the Host Defense Response

In previous publications, it has been shown that Arabidopsis plants with impaired SA and ET signaling display increased susceptibility toward *C. higginsianum*, while JA signaling did not affect disease progression (O'Connell et al., 2004; Liu et al., 2007). A survey of PR gene expression revealed that JA/ET-dependent induction of PR-4 and PDF1.2 occurred earlier than SA-dependent induction of PR-2 and PR-5 in response to *C. higginsianum* (Narusaka et al., 2004), indicating that SA-dependent defense responses might be suppressed by the fungus in favor of the JA response, at least during the early interaction.

We show that free SA progressively accumulates in the course of the Arabidopsis-*C. higginsianum* interaction. In starch-free genotypes, the SA pool was dominated by free SA at 4 dpi, which is regarded as the physiologically active form (for review, see Vlot et al., 2009). While the contents of free SA were elevated 3-fold in the starch-free mutants compared with the wild type at 4 dpi, the transcript accumulation of the SA-dependent PR genes PR-1 and PR-2 was attenuated relative to the wild type, indicating an imbalance between the SA signal and the transcriptional response. The maximum transcript accumulation of the JA/ET-induced PR gene PDF1.2 was also shifted to later time points in the starch-free mutants.

The phytoalexin camalexin is induced in a partially SA-independent fashion, and it has been shown that camalexin-deficient *pad3* mutants are more susceptible toward *C. higginsianum* (Narusaka et al., 2004). Similar to the PR gene induction, the accumulation of camalexin was reduced in the starch-free mutants compared with the wild type. Altogether, these data suggest that the activation of induced defense reactions is slower in *pgm* and *adg1-1*, while the balance between the SA and JA/ET-dependent defense signaling pathways does not seem to be affected in these mutants. Furthermore, our data show that at least the induction of SA-triggered defense responses is negatively modulated by the carbon status of infected leaves.

Observations in the photorespiratory *shmt* mutant (Moreno et al., 2005) and in the peroxisomal catalase mutant *cat2* (Chaouch et al., 2010) strongly support the idea that limited carbon availability can dampen the defense response in Arabidopsis. Likewise, it was recently demonstrated that both basal defense and R gene-mediated defense responses are modulated by the circadian clock regulator CCA1 and occur more strongly during the anticipated light phase, when the availability of carbon building blocks is high, than during the anticipated dark phase, when carbon supply is limited (Wang et al., 2011). Besides the diurnal regulation of carbon-responsive genes, the diurnal oscillation of many circadian clock-regulated genes is altered in the *pgm* mutant (Bläsing et al., 2005). However, diurnal CCA1 oscillation was not substantially affected in *pgm* in comparison with the wild type (Bläsing et al., 2005), making it unlikely that distorted diurnal regulation of CCA1 contributes to the hampered defense responses in the starch-free mutants.

Interestingly, starch accumulated in the immediate vicinity of *C. higginsianum* infection sites during the necrotrophic interaction phase, which temporally and spatially coincided with a reduction in photosynthetic electron transport. These observations indicate that starch synthesis around a developing necrosis is predominantly driven by the import of carbohydrates from distant mesophyll cells, which exhibited increased photosynthetic activity. If we assume that host defense is most pronounced in immediately affected cells close to infection sites, it seems tempting to speculate that starch synthesis driven by imported carbohydrates might generate a buffer of carbon skeletons that is important to enable an efficient local defense response. In this context, the absence of starch mobilization may consequently allow for increased proliferation of the pathogen during the necrotrophic phase.

In this model, the immediately challenged cells represent local sinks for carbon, which is in agreement with the general hypothesis that infected leaf tissue undergoes a source-to-sink transition (Biemelt and Sonnewald, 2006). A local decrease in photosynthetic activity at the infection site and a simultaneous increase in photosynthesis in unaffected leaf areas have also been observed in several biotrophic interactions (Biemelt and Sonnewald, 2006). The local decline in photosynthesis was attributed to the generation of hexoses by apoplastic invertase and the subsequent repression of photosynthetic genes by elevated hexose levels (Scholes et al., 1994), which is also the case in *C. higginsianum*-infected leaves.

The Susceptibility of Starch-Free Mutants toward Hemibiotrophic and Biotrophic Fungi Is Altered in Opposite Ways

In contrast to the interaction with *C. higginsianum*, the attenuated host defense evident in starch-free Arabidopsis mutants does not seem to affect the interaction with the powdery mildew fungus *E. cruciferarum*, as we have observed that the SA-dependent defense response was already very effectively suppressed by *E. cruciferarum*. Both analyzed starch-free mutants displayed a substantially reduced susceptibility toward *E. cruciferarum*, which may simply be explained by limited carbohydrate supply to the biotrophic parasite. Similarly, striped or white leaves of the barley *albostrians* mutant were shown to be more resistant toward the barley powdery mildew fungus *Blumeria*

graminis f. sp. *hordei* (Jain et al., 2004). By contrast, the white leaves of the *albostrians* mutant also displayed hypersusceptibility to the hemibiotrophic fungus *Bipolaris sorokiniana* (Schäfer et al., 2004). This exemplifies that the diurnal carbon availability represents a susceptibility factor that varies in importance depending on the regarded interaction.

MATERIALS AND METHODS

Plant and Fungal Material and Growth Conditions

Arabidopsis (*Arabidopsis thaliana*) plants were grown for 2 weeks in short-day conditions (8 h of light, 22°C/16 h of dark, 20°C) and subsequently grew for 3 weeks in a 12-h/12-h light/dark cycle, or for 2 weeks in a 20-h/4-h light/dark cycle (22°C/20°C), in phytotrons (CLF, Wertingen, Germany) at 110 μE m^{-2} s^{-1} photon flux density, except for MEm4 transgenic plants (see below), which were kept in short-day conditions. Exactly 7 d prior to inoculation with *C. higginsianum*, each plant was fertilized with 20 mL of 0.2% WUXAL-Super fertilizer (Aglukon).

Seeds for *pgm* (N210), *adg1-1* (N3094), *sex1-1* (N3093), the *cca1-11/lhy-21* double mutant (N9809), and the related parental line (N9808) carrying a CCR2:LUC reporter gene fusion (Doyle et al., 2002) were obtained from the Nottingham Arabidopsis Stock Center (University of Nottingham). *tpt1-2* (SALK_073707) seeds were kindly provided by Dr. Frank Ludewig (Institute of Botany, University of Cologne) and Dr. Anja Schneider (Ludwig-Maximilians-University Munich), and MEm4 seeds were kindly provided by Dr. Veronica Maurino (Institute of Botany, University of Cologne; Fahnenstich et al., 2007). All mutants and transformants were in the Col-0 background, except for *cca1-11/lhy-21* and the related parental line, which were in the Wassilewskija-2 background.

Colletotrichum higginsianum isolate MAFF 305635 (kindly provided by the Ministry of Forestry and Fisheries, Japan) was grown on oat meal agar plates (5% [w/v] shredded oat meal, 1.2% [w/v] agar) for 7 d at 22°C under illumination to promote conidia formation.

C. higginsianum Infection Assays

Leaf infection by *C. higginsianum* was performed by spray inoculation with a conidia titer of 2×10^6 conidia mL^{-1} as described by Voll et al. (2012).

Assessment of HR

Leaf cells undergoing HR were scored at 2 dpi by epifluorescence microscopy with a Leica DMR fluorescence microscope using UV excitation and the long-pass emission filter of Leica filter cube A. Per replicate, all appressoria present on one-half of a leaf (commonly between 100 and 300) were assessed, and nine or 10 replicates per genotype were examined.

Erysiphe cruciferarum Infection Assays

Arabidopsis powdery mildew fungus *E. cruciferarum* was propagated on Arabidopsis *pad4* mutants (Glazebrook et al., 1996) in a growth chamber at 22°C and a 10-h photoperiod with 120 μmol m^{-2} s^{-1} light and 65% relative humidity. According to Hoefle et al. (2011), we inoculated 5-week-old Arabidopsis plants with three to five conidia of *E. cruciferarum* per square millimeter of leaf area for scoring disease progression at 6 to 10 d after inoculation.

Assessment of *C. higginsianum* during in Planta Development and Evaluation of Susceptibility

To obtain quantitative data on pathogen presence, an improved protocol as compared with Voll et al. (2012) was followed. A total of 2 cm^2 of leaf material was pooled from leaf punches from at least four different leaves, and the samples were homogenized with mortar and pestle under liquid nitrogen before genomic DNA of *C. higginsianum*-infected leaves was extracted with the Qiagen DNeasy Kit. As an internal control, the plasmid pA7-P19 (Vogel, 2009) was added to the leaf powder. After homogenization in 400 μL of Qiagen buffer AP1, the manufacturer's Plant Mini protocol was followed. Fungal DNA quantity was subsequently analyzed with a Stratagene Mx3000P qPCR System using Brilliant II SYBR Green QPCR Master Mix and the primers already described for the *C. higginsianum* TrpC gene, the Arabidopsis RbcS gene, and the internal control pA7-P19 (Supplemental Table S4). The relative quantity of fungal DNA was then calculated as described by Rieu and Powers (2009) and normalized to RbcS, the internal control, or the leaf sample area. Of the three procedures, normalization to leaf area proved most reproducible in over a dozen experiments and was thus chosen as the standard procedure.

Assessment of *E. cruciferarum* Development and Evaluation of Susceptibility

For the quantitation of *E. cruciferarum* genomic DNA, about 60 mg of leaf material was pooled from at least four different leaves. Extraction and analysis of the samples were performed as described for the quantitation of genomic DNA from *C. higginsianum* using primers for the Arabidopsis RbcS gene and specific primers for a β-tubulin gene of *E. cruciferarum* (Supplemental Table S4).

Determination of Soluble Sugars, Malate, Fumarate, and Starch

Soluble sugars were extracted twice with 80% ethanol from snap-frozen leaves and assayed in a coupled enzymatic assay using a microtiter plate reader as described by Voll et al. (2003). Malate and fumarate were assayed in the same extracts in a microtiter plate reader (BioTek), determining the reduction of NAD^+ at 340 nm in a coupled enzymatic assay based on Lowry and Passonneau (1993). Malate was converted to oxaloacetate by the addition of 2 units of malate dehydrogenase (Sigma M1567) in a 200 mM hydrazine buffer (pH 9.1) containing 2 mM NAD^+, yielding oxaloacetate hydrazone. After complete turnover of malate, 1 unit of fumarase was added to the mixture to couple fumarate conversion to the assay. Starch was assayed from ethanol-insoluble leaf material as described by Voll et al. (2003). Iodine staining of starch was conducted as described by Kofler et al. (2000).

Determination of Free SA, SAG, and Camalexin

Free SA, SAG, and camalexin were extracted and analyzed as described (Voll et al., 2012) with minor modifications. A total of 2 cm^2 of leaf material was punched out with a cork borer, supplemented with 250 ng of *o*-anisic acid (Acros Organics) as an internal standard, and extracted once with 600 μL of 70% methanol at 65°C for 1 h and once with 600 μL of 90% methanol at 65°C for 1 h. The solvent of the combined extracts was then evaporated with a vacuum concentrator, followed by a precipitation step with 500 μL of 5% (w/v) TCA. Free phenols and camalexin were partitioned two times against 600 μL of cyclohexane:ethyl acetate (1:1). The combined organic phases were evaporated and resuspended in 400 μL of 20% acetonitrile in 25 mM KH_2PO_4 (pH 2.6). The remaining aqueous phase was acidified with 1 volume of 8 M HCl and incubated at 80°C for 1 h. After partitioning as above, the organic phase was supplemented with 20 μL of 20% acetonitrile in 25 mM KH_2PO_4 (pH 2.6) to prevent sublimation of SA, evaporated, and resuspended in 400 μL of 20% acetonitrile in 25 mM KH_2PO_4 (pH 2.6), to give the HPLC starting mobile phase.

HPLC separation of SA, *o*-anisic acid, and camalexin was performed on a Dionex Summit system (P680, ASI-100, TCC-100, RF-2000) equipped with a Phenomenex Luna Security Guard C18 column (4.0 × 3.0 mm) followed by a 5-μm Luna C18(2) reverse-phase column (250 × 4.6 mm) as described by Voll et al. (2012).

Northern-Blot Analysis of PR Genes

Northern-blot analysis of PR gene transcript accumulation was conducted as described previously (Voll et al., 2012), employing probes generated by PCR using the primer combinations given in Supplemental Table S4.

Statistical Analysis

Student's *t* tests were performed with SigmaPlot 12 (Systat Software) after testing for normality (Shapiro-Wilk test) and equal variance.

Supplemental Data

The following materials are available in the online version of this article.

Supplemental Figure S1. Infection cycle of *C. higginsianum* on Arabidopsis leaves.

Supplemental Figure S2. Carbon partitioning in *C. higginsianum*-infected leaves.

Supplemental Figure S3. Photosynthetic performance of *C. higginsianum*-infected leaves.

Supplemental Figure S4. Schematic illustration of leaf carbohydrate metabolism in Arabidopsis.

Supplemental Figure S5. Major carbohydrate contents in mock- and *C. higginsianum*-infected leaves at 3.5 and 4 dpi.

Supplemental Figure S6. Correlation analysis of carbohydrate accumulation in mock-treated plants during the light phase and susceptibility to *C. higginsianum* at 4 dpi.

Supplemental Figure S7. Correlation analysis of carbohydrate content dynamics between infected and mock-treated plants and susceptibility to *C. higginsianum* at 4 dpi.

Supplemental Table S1. Starch and soluble sugar contents in Arabidopsis leaves after extended darkness.

Supplemental Table S2. Soluble sugar and starch contents of *cca1/lhy*.

Supplemental Table S3. Soluble sugar, starch, malate, and fumarate contents of MEm4 in 12-h/12-h and 8-h/16-h light/dark cycles.

Supplemental Table S4. Primers used in this study.

Supplemental Materials and Methods S1.

ACKNOWLEDGMENTS

We thank Frank Ludewig, Rainer Häusler (both Institute of Botany, University of Cologne), and Anja Schneider (Ludwig-Maximilians-University Munich) for generous provision of *tpt1-2* seeds as well as Veronica Maurino (Institute of Developmental and Molecular Biology of Plants, University of Düsseldorf) for providing MEm4 seeds. We also appreciate the skillful technical assistance of Alexandra Ammon and we are very grateful to Stephen Reid (both Friedrich-Alexander-University Erlangen-Nuremberg) for editing language and style of the manuscript.

Received October 23, 2012; accepted March 12, 2013; published March 13, 2013.

LITERATURE CITED

Bechinger C, Giebel K-F, Schnell M, Leiderer P, Deising HB, Bastmeyer M (1999) Optical measurements of invasive forces exerted by appressoria of a plant pathogenic fungus. Science **285:** 1896–1899

Berger S, Papadopoulos M, Schreiber U, Kaiser W, Roitsch T (2004) Complex regulation of gene expression, photosynthesis and sugar levels by pathogen infection in tomato. Physiol Plant **122:** 419–428

Biemelt S, Sonnewald U (2006) Plant-microbe interactions to probe regulation of plant carbon metabolism. J Plant Physiol **163:** 307–318

Birker D, Heidrich K, Takahara H, Narusaka M, Deslandes L, Narusaka Y, Reymond M, Parker JE, O'Connell R (2009) A locus conferring resistance to *Colletotrichum higginsianum* is shared by four geographically distinct Arabidopsis accessions. Plant J **60:** 602–613

Bläsing OE, Gibon Y, Günther M, Höhne M, Morcuende R, Osuna D, Thimm O, Usadel B, Scheible W-R, Stitt M (2005) Sugars and circadian regulation make major contributions to the global regulation of diurnal gene expression in *Arabidopsis*. Plant Cell **17:** 3257–3281

Both M, Csukai M, Stumpf MPH, Spanu PD (2005) Gene expression profiles of *Blumeria graminis* indicate dynamic changes to primary metabolism during development of an obligate biotrophic pathogen. Plant Cell **17:** 2107–2122

Caspar T, Huber SC, Somerville C (1985) Alterations in growth, photosynthesis, and respiration in a starchless mutant of *Arabidopsis thaliana* (L.) deficient in chloroplast phosphoglucomutase activity. Plant Physiol **79:** 11–17

Caspar T, Lin T-P, Kakefuda G, Benbow L, Preiss J, Somerville C (1991) Mutants of Arabidopsis with altered regulation of starch degradation. Plant Physiol **95:** 1181–1188

Cecchini NM, Monteoliva MI, Alvarez ME (2011) Proline dehydrogenase contributes to pathogen defense in Arabidopsis. Plant Physiol **155:** 1947–1959

Chaouch S, Queval G, Vanderauwera S, Mhamdi A, Vandorpe M, Langlois-Meurinne M, Van Breusegem F, Saindrenan P, Noctor G (2010) Peroxisomal hydrogen peroxide is coupled to biotic defense responses by ISOCHORISMATE SYNTHASE1 in a daylength-related manner. Plant Physiol **153:** 1692–1705

Chen L-Q, Hou B-H, Lalonde S, Takanaga H, Hartung ML, Qu X-Q, Guo W-J, Kim J-G, Underwood W, Chaudhuri B, et al (2010) Sugar transporters for intercellular exchange and nutrition of pathogens. Nature **468:** 527–532

Chen L-Q, Qu X-Q, Hou B-H, Sosso D, Osorio S, Fernie AR, Frommer WB (2012) Sucrose efflux mediated by SWEET proteins as a key step for phloem transport. Science **335:** 207–211

Chou H-M, Bundock N, Rolfe SA, Scholes JD (2000) Infection of *Arabidopsis thaliana* leaves with *Albugo candida* (white blister rust) causes a reprogramming of host metabolism. Mol Plant Pathol **1:** 99–113

Deising HB, Werner S, Wernitz M (2000) The role of fungal appressoria in plant infection. Microbes Infect **2:** 1631–1641

Divon HH, Fluhr R (2007) Nutrition acquisition strategies during fungal infection of plants. FEMS Microbiol Lett **266:** 65–74

Doehlemann G, Wahl R, Horst RJ, Voll LM, Usadel B, Poree F, Stitt M, Pons-Kühnemann J, Sonnewald U, Kahmann R, et al (2008) Reprogramming a maize plant: transcriptional and metabolic changes induced by the fungal biotroph *Ustilago maydis*. Plant J **56:** 181–195

Doyle MR, Davis SJ, Bastow RM, McWatters HG, Kozma-Bognár L, Nagy F, Millar AJ, Amasino RM (2002) The ELF4 gene controls circadian rhythms and flowering time in *Arabidopsis thaliana*. Nature **419:** 74–77

Fahnenstich H, Saigo M, Niessen M, Zanor MI, Andreo CS, Fernie AR, Drincovich MF, Flügge U-I, Maurino VG (2007) Alteration of organic acid metabolism in Arabidopsis overexpressing the maize C4 NADP-malic enzyme causes accelerated senescence during extended darkness. Plant Physiol **145:** 640–652

Fotopoulos V, Gilbert MJ, Pittman JK, Marvier AC, Buchanan AJ, Sauer N, Hall JL, Williams LE (2003) The monosaccharide transporter gene, *AtSTP4*, and the cell-wall invertase, *Atβfruct1*, are induced in Arabidopsis during infection with the fungal biotroph *Erysiphe cichoracearum*. Plant Physiol **132:** 821–829

Foyer CH, Noctor G (2005) Oxidant and antioxidant signalling in plants: a re-evaluation of the concept of oxidative stress in a physiological context. Plant Cell Environ **28:** 1056–1071

Glawischnig E (2007) Camalexin. Phytochemistry **68:** 401–406

Glazebrook J, Rogers EE, Ausubel FM (1996) Isolation of Arabidopsis mutants with enhanced disease susceptibility by direct screening. Genetics **143:** 973–982

Graf A, Schlereth A, Stitt M, Smith AM (2010) Circadian control of carbohydrate availability for growth in Arabidopsis plants at night. Proc Natl Acad Sci USA **107:** 9458–9463

Herbers K, Meuwly P, Frommer WB, Metraux JP, Sonnewald U (1996) Systemic acquired resistance mediated by the ectopic expression of invertase: possible hexose sensing in the secretory pathway. Plant Cell **8:** 793–803

Hiruma K, Onozawa-Komori M, Takahashi F, Asakura M, Bednarek P, Okuno T, Schulze-Lefert P, Takano Y (2010) Entry mode-dependent function of an indole glucosinolate pathway in *Arabidopsis* for nonhost resistance against anthracnose pathogens. Plant Cell **22:** 2429–2443

Hoefle C, Huesmann C, Schultheiss H, Börnke F, Hensel G, Kumlehn J, Hückelhoven R (2011) A barley ROP GTPase ACTIVATING PROTEIN associates with microtubules and regulates entry of the barley powdery mildew fungus into leaf epidermal cells. Plant Cell **23:** 2422–2439

Horsfall JG, Dimond AE (1957) Interactions of tissue sugar, growth substances and disease susceptibility. Z Pflanzenkr Pflanzenschutz **64:** 415–421

Horst RJ, Engelsdorf T, Sonnewald U, Voll LM (2008) Infection of maize leaves with *Ustilago maydis* prevents establishment of C4 photosynthesis. J Plant Physiol **165:** 19–28

Jain SK, Langen G, Hess W, Börner T, Hückelhoven R, Kogel K-H (2004) The white barley mutant albostrians shows enhanced resistance to the biotroph *Blumeria graminis* f. sp. *hordei*. Mol Plant Microbe Interact **17:** 374–382

Kleemann J, Rincon-Rivera LJ, Takahara H, Neumann U, Ver Loren van Themaat E, van der Does HC, Hacquard S, Stüber K, Will I, Schmalenbach W, et al (2012) Sequential delivery of host-induced virulence effectors by appressoria and intracellular hyphae of the phytopathogen *Colletotrichum higginsianum*. PLoS Pathog **8:** e1002643

Kofler H, Häusler RE, Schulz B, Gröner F, Flügge UI, Weber A (2000) Molecular characterisation of a new mutant allele of the plastid phosphoglucomutase in Arabidopsis, and complementation of the mutant with the wild-type cDNA. Mol Gen Genet **263:** 978–986

Lee E-J, Matsumura Y, Soga K, Hoson T, Koizumi N (2007) Glycosyl hydrolases of cell wall are induced by sugar starvation in Arabidopsis. Plant Cell Physiol **48:** 405–413

Lin T-P, Caspar T, Somerville C, Preiss J (1988) Isolation and characterization of a starchless mutant of *Arabidopsis thaliana* (L.) Heynh lacking ADPglucose pyrophosphorylase activity. Plant Physiol **86:** 1131–1135

Liu G, Kennedy R, Greenshields DL, Peng G, Forseille L, Selvaraj G, Wei Y (2007) Detached and attached Arabidopsis leaf assays reveal distinctive defense responses against hemibiotrophic *Colletotrichum* spp. Mol Plant Microbe Interact **20:** 1308–1319

Lowry OH, Passonneau JV (1993) Enzymatic Analysis: A Practical Guide. Humana Press, Totowa, NJ

Mendgen K, Hahn M (2002) Plant infection and the establishment of fungal biotrophy. Trends Plant Sci **7:** 352–356

Moreno JI, Martín R, Castresana C (2005) Arabidopsis SHMT1, a serine hydroxymethyltransferase that functions in the photorespiratory pathway influences resistance to biotic and abiotic stress. Plant J **41:** 451–463

Münch S, Lingner U, Floss DS, Ludwig N, Sauer N, Deising HB (2008) The hemibiotrophic lifestyle of *Colletotrichum* species. J Plant Physiol **165:** 41–51

Narusaka Y, Narusaka M, Park P, Kubo Y, Hirayama T, Seki M, Shiraishi T, Ishida J, Nakashima M, Enju A, et al (2004) RCH1, a locus in Arabidopsis that confers resistance to the hemibiotrophic fungal pathogen *Colletotrichum higginsianum*. Mol Plant Microbe Interact **17:** 749–762

O'Connell R, Herbert C, Sreenivasaprasad S, Khatib M, Esquerré-Tugayé M-T, Dumas B (2004) A novel Arabidopsis-*Colletotrichum* pathosystem for the molecular dissection of plant-fungal interactions. Mol Plant Microbe Interact **17:** 272–282

O'Connell RJ, Thon MR, Hacquard S, Amyotte SG, Kleemann J, Torres MF, Damm U, Buiate EA, Epstein L, Alkan N, et al (2012) Lifestyle transitions in plant pathogenic *Colletotrichum* fungi deciphered by genome and transcriptome analyses. Nat Genet **44:** 1060–1065

Parker D, Beckmann M, Zubair H, Enot DP, Caracuel-Rios Z, Overy DP, Snowdon S, Talbot NJ, Draper J (2009) Metabolomic analysis reveals a common pattern of metabolic re-programming during invasion of three host plant species by *Magnaporthe grisea*. Plant J **59:** 723–737

Pavet V, Olmos E, Kiddle G, Mowla S, Kumar S, Antoniw J, Alvarez ME, Foyer CH (2005) Ascorbic acid deficiency activates cell death and disease resistance responses in Arabidopsis. Plant Physiol **139:** 1291–1303

Rieu I, Powers SJ (2009) Real-time quantitative RT-PCR: design, calculations, and statistics. Plant Cell **21:** 1031–1033

Schäfer P, Hückelhoven R, Kogel K-H (2004) The white barley mutant *albostrians* shows a supersusceptible but symptomless interaction phenotype with the hemibiotrophic fungus *Bipolaris sorokiniana*. Mol Plant Microbe Interact **17:** 366–373

Scharte J, Schön H, Weis E (2005) Photosynthesis and carbohydrate metabolism in tobacco leaves during an incompatible interaction with *Phytophthora nicotianae*. Plant Cell Environ **28:** 1421–1435

Schneider A, Häusler RE, Kolukisaoglu Ü, Kunze R, van der Graaff E, Schwacke R, Catoni E, Desimone M, Flügge U-I (2002) An *Arabidopsis thaliana* knock-out mutant of the chloroplast triose phosphate/phosphate translocator is severely compromised only when starch synthesis, but not starch mobilisation is abolished. Plant J **32:** 685–699

Scholes JD, Lee PJ, Horton P, Lewis DH (1994) Invertase: understanding changes in the photosynthetic and carbohydrate metabolism of barley leaves infected with powdery mildew. New Phytol **126:** 216–222

Shimada C, Lipka V, O'Connell R, Okuno T, Schulze-Lefert P, Takano Y (2006) Nonhost resistance in Arabidopsis-*Colletotrichum* interactions acts at the cell periphery and requires actin filament function. Mol Plant Microbe Interact **19:** 270–279

Stergiopoulos I, de Wit PJGM (2009) Fungal effector proteins. Annu Rev Phytopathol **47:** 233–263

Struck C, Ernst M, Hahn M (2002) Characterization of a developmentally regulated amino acid transporter (AAT1p) of the rust fungus *Uromyces fabae*. Mol Plant Pathol **3:** 23–30

Struck C, Mueller E, Martin H, Lohaus G (2004) The *Uromyces fabae UfAAT3* gene encodes a general amino acid permease that prefers uptake of *in planta* scarce amino acids. Mol Plant Pathol **5:** 183–189

Stuttmann J, Hubberten H-M, Rietz S, Kaur J, Muskett P, Guerois R, Bednarek P, Hoefgen R, Parker JE (2011) Perturbation of *Arabidopsis* amino acid metabolism causes incompatibility with the adapted biotrophic pathogen *Hyaloperonospora arabidopsidis*. Plant Cell **23:** 2788–2803

Swarbrick PJ, Schulze-Lefert P, Scholes JD (2006) Metabolic consequences of susceptibility and resistance (race-specific and broad-spectrum) in barley leaves challenged with powdery mildew. Plant Cell Environ **29:** 1061–1076

Thimm O, Bläsing O, Gibon Y, Nagel A, Meyer S, Krüger P, Selbig J, Müller LA, Rhee SY, Stitt M (2004) MAPMAN: a user-driven tool to display genomics data sets onto diagrams of metabolic pathways and other biological processes. Plant J **37:** 914–939

Thines E, Weber RWS, Talbot NJ (2000) MAP kinase and protein kinase A-dependent mobilization of triacylglycerol and glycogen during appressorium turgor generation by *Magnaporthe grisea*. Plant Cell **12:** 1703–1718

Usadel B, Bläsing OE, Gibon Y, Retzlaff K, Höhne M, Günther M, Stitt M (2008) Global transcript levels respond to small changes of the carbon status during progressive exhaustion of carbohydrates in Arabidopsis rosettes. Plant Physiol **146:** 1834–1861

Vlot AC, Dempsey DA, Klessig DF (2009) Salicylic acid, a multifaceted hormone to combat disease. Annu Rev Phytopathol **47:** 177–206

Voegele RT, Struck C, Hahn M, Mendgen K (2001) The role of haustoria in sugar supply during infection of broad bean by the rust fungus *Uromyces fabae*. Proc Natl Acad Sci USA **98:** 8133–8138

Vogel F (2009) Molekulare Analyse des Makromolekültransports in Pflanzen anhand eines viralen Transportproteins. PhD thesis. Friedrich-Alexander-Universität Erlangen-Nürnberg, Erlangen, Germany

Voll L, Häusler RE, Hecker R, Weber A, Weissenböck G, Fiene G, Waffenschmidt S, Flügge U-I (2003) The phenotype of the Arabidopsis *cue1* mutant is not simply caused by a general restriction of the shikimate pathway. Plant J **36:** 301–317

Voll LM, Zell MB, Engelsdorf T, Saur A, Wheeler MG, Drincovich MF, Weber APM, Maurino VG (2012) Loss of cytosolic NADP-malic enzyme 2 in *Arabidopsis thaliana* is associated with enhanced susceptibility to *Colletotrichum higginsianum*. New Phytol **195:** 189–202

Wahl R, Wippel K, Goos S, Kämper J, Sauer N (2010) A novel high-affinity sucrose transporter is required for virulence of the plant pathogen *Ustilago maydis*. PLoS Biol **8:** e1000303

Wang W, Barnaby JY, Tada Y, Li H, Tör M, Caldelari D, Lee DU, Fu X-D, Dong X (2011) Timing of plant immune responses by a central circadian regulator. Nature **470:** 110–114

Yu T-S, Kofler H, Häusler RE, Hille D, Flügge U-I, Zeeman SC, Smith AM, Kossmann J, Lloyd J, Ritte G, et al (2001) The *Arabidopsis sex1* mutant is defective in the R1 protein, a general regulator of starch degradation in plants, and not in the chloroplast hexose transporter. Plant Cell **13:** 1907–1918

Zell MB, Fahnenstich H, Maier A, Saigo M, Voznesenskaya EV, Edwards GE, Andreo C, Schleifenbaum F, Zell C, Drincovich MF, et al (2010) Analysis of Arabidopsis with highly reduced levels of malate and fumarate sheds light on the role of these organic acids as storage carbon molecules. Plant Physiol **152:** 1251–1262